LRP 351/88 July 1988

PROSPECTS FOR HIGH POWER QUASI-OPTICAL GYROTRONS OPERATING IN THE MILLIMETER WAVE RANGE

T.M. Tran, M.Q. Tran, S. Alberti, J.P. Hogge,
B. Isaak, P. Muggli and A. Perrenoud

Prospects for High Power Quasi-Optical Gyrotrons Operating in the Millimeter Wave Range

T.M. Tran, M.Q. Tran, S. Alberti, J.P. Hogge,
B. Isaak, P. Muggli and A. Perrenoud

Centre de Recherches en Physique des Plasmas
Association Euratom-Confédération Suisse
Ecole Polytechnique Fédérale de Lausanne

The prospects for high power (several megawatts) quasi-optical gyrotrons operating in the high frequency region ($\geq$ 150 GHz) are considered. The analysis is mainly concerned with the physics of interaction between the annular electron beam and the electromagnetic field within the quasi-optical resonator, together with the constraints required by long-pulse or cw operations. It is shown that powers of several megawatts at frequencies exceeding 150 GHz are possible if one can maintain single mode operation in the overmoded quasi-optical resonators. A thorough performance study of the magnetron injection gun (MIG) for such high power gyrotrons, is also carried out, using the adiabatic theory as well as the numerical simulations.

I. Introduction

In the past decade, intensive research has been conducted on high-power gyrotron oscillators for application to fusion device heating at the millimeter wavelengths (Electron Cyclotron Resonance Heating). Recently, conventional gyrotrons which utilize a closed cylindrical cavity as the resonant structure, have achieved 100 kW cw operation at 140 GHz [1] and 645 kW short pulse operation at frequencies step-tunable between 126 and 243 GHz [2]. An alternative millimeter source of high-power radiation is the gyrotron which utilizes the quasi-optical resonator. Devices based on this concept have the potentialities of operating at very high frequencies [3].

In this paper, the prospects of quasi-optical gyrotrons capable of producing high power (several megawatts) radiation at the millimeter wave range are examined. The analysis is based essentially on the physics of interaction between the annular electron beam (produced by the MIG) and the TEM_{oo} Gaussian radiation field; the technological constraints on the beam and the resonator are also taken into account, as required by cw operations. The physics of interaction is mainly contained in the dependency of the interaction efficiency on two reduced parameters which are defined in terms of the beam and resonator parameters. By expressing the ohmic loss constraint and the beam voltage depression in terms of these parameters, a set of design equations are obtained. A parametric analysis can then be performed in the permissible design space in order to examine the power capabilities of quasi-optical gyrotrons. The analysis indicates that the electron beam should have a small radius in order to interact efficiently with the finite size radiation beam. As a consequence, the electron beam should be rather thick in high power quasi-optical gyrotrons. In order to verify that the beam quality is not degraded by such a requirement, a gun design study has also been conducted for a 1 MW, 150 GHz gyrotron, using the adiabatic theory and a trajectory simulation code.

This paper is organized as follows. The design model is outlined in section II. The parametric analysis, that is based on this model, follows in section III. Operations at 150 and 280 GHz are considered. Section IV is devoted to the design of the MIG for a 150 GHz, 1 MW quasi-optical gyrotron oscillator while the magnet system is considered in section V. Finally, section VI concludes the paper.

II. Design Model

In this section, a nonlinear model of the interaction between the electron beam and the single mode r.f. field in a quasi-optical resonator will be described. The constraints imposed by the ohmic heating of the mirrors as well as the D.C. space charge effects (or beam voltage depression) will be also considered. The nonlinear model, together with these constraints will be used later to perform an extensive parametric analysis of the high power ($\geq$ 1 MW) quasi-optical gyrotron operating at the millimeter wave range.

1. Single mode efficiency

Assuming a TEM_{oo} Gaussian mode in the quasi-optical resonator given by the following electric field profile:

$$E(z) = E_o e^{-z^2/w_o^2}, \tag{1}$$

where the z-axis is along the electron beam propagation, E_o and w_o are respectively the electric field and the spot size at the radiation beam waist $z = 0$, it can be shown [4–6] that the efficiency of energy extraction from the perpendicular component of the pencil electron beam (or perpendicular efficiency) $\eta_\perp$ depends only on the normalized field amplitude F, the normalized interaction length μ and the detuning parameter Δ defined by:

$$F = \frac{E_o \beta_\perp{}^{-3}}{cB_o} \simeq \frac{eE_o}{mc^2 k} \beta_\perp{}^{-3}, \tag{2.a}$$

$$\mu = \frac{\beta_\perp{}^2}{\beta_\parallel} k w_o, \tag{2.b}$$

$$\Delta = \frac{2}{\beta_\perp{}^2}\left(1 - \frac{\Omega_o}{\gamma\omega}\right). \tag{2.c}$$

In Eqs.(2), $\beta_\perp$ and $\beta_\parallel$ are respectively the perpendicular and the parallel components of the electron velocity normalized to the speed of light, α is the velocity ratio $\beta_\perp/\beta_\parallel$, $\gamma = (1 - {\beta_\perp}^2 - {\beta_\parallel}^2)^{-1/2}$ is the relativistic factor, $\Omega_o = eB_o/m$ is the non-relativistic electron cyclotron frequency and $\omega = ck$ is the r.f. angular frequency. The optimum perpendicular efficiency $\eta_\perp$ with respect to the detuning parameter Δ can be determined numerically [4–6] and is conveniently represented as contour plots on the (F, μ) plane shown in Fig.(1). It should be noted that this result was obtained, assuming a pencil electron beam [6]. In this paper, the value of $\eta_\perp$ of an annular beam will be assumed to be half of that of a pencil beam. This assumption, which is correct in the small-signal regime [7], underestimates somewhat the maximum nonlinear efficiency that can be obtained from the annular beam in a quasi-optical resonator [8].

2. Ohmic heating of the mirrors

A major constraint in a cw gyrotron is the constraint on the average ohmic heating ρ_{ohm} of the resonator mirrors. This can be calculated by integrating the r.f. power flow on the mirror and dividing by the mirror area. In terms of the normalized field amplitude F, ρ_{ohm} can then be written as:

$$\rho_{\text{ohm}}\,[\text{kW/cm}^2] = 634\,\sigma^{-1/2} f^{5/2}(1+g)\gamma^2 {\beta_\perp}^6 F^2, \tag{3}$$

where σ is the electrical conductivity of the mirror, f is the r.f. frequency expressed in GHz and g is the curvature parameter of the mirror defined as:

$$g = 1 - \frac{d}{R}, \tag{4}$$

with d and R being respectively the mirror separation and the mirror radius of curvature. It has been assumed that the resonator is symmetrical (identical mirrors). For a given frequency f, it is interesting to note that the relation (3) implies that the ohmic heating density ρ_{ohm} increases with increasing beam voltage and increasing electron perpendicular velocity $\beta_\perp$. This relation also shows the necessity of using a near concentric resonator (g close to -1) in high frequency operation. This type of resonator is very close to the line that separates stable and unstable resonators, and hence, requires very critical tolerances in mirror fabrication and alignment in order to obtain stable operation.

The limitations introduced by the ohmic heating constraint are summarized graphically in Fig.(2), where $f = 150$ GHz, $\sigma = 3.6 \times 10^7\,\Omega^{-1}\mathrm{m}^{-1}$ (OHFC copper at 200° C) and $\rho_{\mathrm{ohm}} < 1.5\,\mathrm{kW/cm}^2$. Note that this conservative value of ρ_{ohm} does not take into account any anomalous effect on the AC resistivity at high frequency. In practice, the actual value ofρ_{ohm} could be two to three times as high. For a confocal resonator ($g = 0$) and $\alpha = \beta_\perp/\beta_\parallel = 1.5$, operating at $F = 0.12$ would require a beam voltage lower than 62 kV, in order to obtain $\eta_\perp = 0.7/2 = 0.35$. This maximum voltage can be increased however to 80 kV for a $g = -0.5$ resonator. Alternatively, it can be increased by operating at lower $\eta_\perp$(lower F) or lower α; this could be required at very high frequency gyrotrons.

3. Voltage depression (DC space charge)

The second major constraint for high power gyrotrons is the electron beam voltage depression [9]. Assuming that the beam has a mean radius R_e, a thickness Δ_e and that it is transported to the interaction region through a beam tunnel of radius R_w, the maximum equilibrium current is given by [10]

$$I_{\mathrm{MAX}}\,[\mathrm{A}] = 1.71 \times\, 10^4 \,\frac{\gamma_o \left[1 - (1 - \beta_{\parallel o}^2)^{1/3}\right]^{3/2}}{G(R_e/R_w, \Delta_e/R_w)}, \tag{5}$$

where the subscript "o" refers to the characteristics of the beam *without voltage depression.* The geometrical factor G can be approximated by:

$$G = \frac{3}{4}\frac{\Delta_e}{R_e} + 2\ln\left[\frac{R_w/R_e}{1 + \Delta_e/R_e}\right]. \tag{6}$$

The limiting electron beam power, deduced from Eq.(5) is plotted versus the beam voltage in Fig.(3) for $R_e/R_w = 0.7$, $\Delta_e/R_e = 0$. It can be seen that a multimegawatt gyrotron (at any frequency) would require a beam voltage higher than 90 kV if one would like to operate at modest I/I_{MAX} and at high efficiency ($\eta_\perp \geq 0.3, \alpha \geq 1.5$). Placing the beam closer to the wall of the beam duct would somewhat decrease the minimum required voltage, but the beam interception may become critical.

For a beam current I smaller than I_{MAX}, the electrons suffer a voltage drop (due to their own DC space charge) which is given by:

$$\Delta V\,[\mathrm{kV}] = 30\,\frac{I}{\beta_\parallel} G(R_e/R_w, \Delta_e/R_w), \tag{7}$$

where I is expressed in Amperes. The electron velocities at the interaction region can be related to their upstream (without voltage depression) values by

$$\gamma\beta_\perp = \gamma_o \beta_{\perp o}, \tag{8.a}$$

$$\beta_\parallel{}^2 = 1 - 1/\gamma^2 - \beta_\perp{}^2 = 1 - (1 + \gamma_o^2 \beta_{\perp o}^2)/\gamma^2. \tag{8.b}$$

The equation (8.b) shows that the parallel velocity $\beta_\parallel$ is reduced by the voltage depression: operating too close to I_{MAX} can enhance greatly the potential of mirroring, unless the electron beam has a small spread in $\beta_{\perp o}$. In the parametric analysis that will be presented in section III, the Eqs.(7–8) will be taken into account in order to calculate the correct beam velocities $\beta_\perp$, $\beta_\parallel$ and energy γ in the interaction region.

4. Symmetrical quasi-optical resonators

In the design of resonators for quasi-optical gyrotrons, the most relevant dimensionless parameters [11] are the mirror separation parameter d/λ, the curvature parameter g already defined in Eq.(4) and the round-trip fractional loss T. In terms of these parameters, the radiation spot size at the radiation beam waist (located at the center of the symmetrical resonator) is expressed as:

$$kw_o = \left[2\pi \frac{d}{\lambda}\sqrt{\frac{1+g}{1-g}}\right]^{1/2}. \tag{9}$$

From Eq.(2.b), the normalized interaction length μ can then be written as:

$$\mu = \frac{\beta_\perp{}^2}{\beta_\parallel}\left[2\pi \frac{d}{\lambda}\sqrt{\frac{1+g}{1-g}}\right]^{1/2}. \tag{10}$$

This relation shows a strong trade-off between a near-concentric resonator $g \simeq -1$ (in order to minimize the ohmic heating) and designing a resonator with a small d/λ (in order to minimize the mode competition [7,12]). Operating at higher beam voltage would not help because the ohmic heating constraint would require a g value even closer to -1 as can be seen from Eq.(3) or Fig.(2).

The round-trip transmission loss T is essentially determined by the chosen r.f. output coupling scheme. The output microwave power can then be expressed in terms of F and μ as:

$$P\ [\mathrm{MW}] = 272\,\gamma^2 {\beta_{\parallel}}^2 {\beta_{\perp}}^2 \left[1/\sqrt{1-T} - 1\right] F^2 \mu^2. \tag{11}$$

In the parametric analysis which will be presented later, this relation will be used to determine the required round-trip loss T, assuming that the r.f. power produced by the electron beam is given by:

$$P\ [\mathrm{MW}] = \eta I V_c = 0.256\,\gamma {\beta_{\perp}}^2 I \eta_{\perp}(F, \mu), \tag{12}$$

with I (in A), γ, $\beta_{\perp}$ and $\eta_{\perp}$ obtained consistently from the isoefficiencies shown in Fig.(1) together with the ohmic as well as the voltage depression constraints discussed previously.

III. Parametric Analysis

The primary goal of the parametric analysis, presented in this section, is to determine the beam and resonator parameters for a cw quasi-optical gyrotron at a selected frequency and a desired output power. The isoefficiency curves, shown in Fig.(1) together with the constraints outlined in the previous section will be used. In addition, the parametric analysis assumes the following restrictions in the operating parameters space:

a) Because we want a high perpendicular efficiency *and* a high output power, an optimum choice would be a lowest possible field amplitude F, in order to operate at a high beam voltage which is consistent with the ohmic constraint [see Fig.(2)]. This results in choosing $F = 0.12$ and $\mu = 17$, yielding a perpendicular efficiency $\eta_{\perp} = 0.7/2 = 0.35$ for an annular electron beam. Note that for this operating point, the current is above the starting current at the optimum magnetic field field and thus corresponds to the region of hard excitation [5]. As a consequence, one has to bring the gyrotron from the soft excitation to the hard excitation by adjusting the parameters. It has also been shown, using a multimode numerical simulation [7] that a strong decreasing magnetic field in the interaction space could favor modes with frequency higher than all the linearly unstable modes and could thus provide another method to obtain high efficiency single mode equilibrium.

b) The value of $\alpha = 1.5$ is selected in the parametric analysis. This value is a compromise between having a reasonable perpendicular electron energy and a high limiting beam power [see Fig.(3)].

c) The ohmic power density deposited on the resonator mirrors ρ_{ohm} is assumed to be 1.5 kW/cm^2 with $\sigma = 3.6 \times 10^7 \Omega^{-1}\mathrm{m}^{-1}$ (OHFC copper at 200° C).

d) The ratio of the beam radius to the beam duct radius is taken to be $R_e/R_w = 0.7$ to minimize the DC space charge effects within the beam.

The working equations considered in the analysis are Eqs.(3), (7) and (8). For a given frequency and assigning numerical values for $\eta_\perp$, F, μ, α, σ, ρ_{ohm} and R_e/R_w as specified above, these equations can be solved to yield g, γ, $\beta_\perp$, I and ΔV as functions of two variables: the cathode voltage V_c and I/I_{MAX}. Then, using Eq.(12), one can eliminate V_c in these functions. Finally, using Eqs.(10,11) to determine respectively the mirror spacing parameter d/λ and the resonator transmission T, it becomes possible to obtain the beam parameters V_c, I and the resonator parameters g, d/λ, T as functions of the output power P *for a given* I/I_{MAX}. The results of these calculations are shown in Figs.(4) for $f = 150$ GHz and in Figs.(5) for $f = 280$ GHz for three values of I/I_{MAX}. Figures (4.a,b) and (5.a,b) indicate that the cathode voltage and the beam current should be increased simultaneously in order to achieve high power operation. In addition, it is difficult to maintain a low I/I_{MAX} (lower than 0.1) for a multi-megawatt device, unless it is possible to increase the cathode voltage to several hundreds of kilovolts. However, Fig.(4.c) and Fig.(5.c) show that, in that case, the resonator becomes very close to an unstable concentric one ($g \approx -1$) with a low transmission coefficient as can be seen in Fig.(4.e) and Fig.(5.e).

If the selected curvature parameter is restricted to $g > -0.95$, this study indicates that the maximum power for a 150 GHz quasi-optical gyrotron is about 10 MW, while a 280 GHz gyrotron can still output about 3 MW. However, if the ohmic density ρ_{ohm} is allowed to increase beyond $1.5\,\text{kW/cm}^2$, then a dramatic increase of these maximum powers could be achieved.

To conclude this section, three designs are given in Table 1, based on the results of the parametric analysis. The second column shows that the increase in frequency requires an increase of d/λ, which means that the longitudinal mode competition might be severe in very high frequency operations. A comparison between the first and the third columns indicates that an increase in output power can be achieved with a slight increase in beam voltage and a large increase in the beam current, resulting in a larger voltage depression. Fortunately, this depression is still modest since the total efficiency $\eta = P/IV_c$ is only weakly degraded in that case.

IV. Magnetron Injection Gun (MIG) for a 150 GHz, 1 MW Gyrotron

1. *Adiabatic theory.*

With the electron beam performances in the interaction region deduced from the previously described design considerations, the adiabatic theory [13] can provide very useful informations for the design of the magnetron injection gun. The obtained estimates will be used later in the numerical simulation to obtain a finer gun design.

Assuming adiabatic flow and neglecting space charge effects within the gun emitter, a relation between the electric field at the cathode E_k and the electron velocities in the interaction region [13] can be expressed as:

$$E_k \text{ [kV/cm]} = 107\,\gamma^2\beta_\perp f[\text{GHz}]/g_c^{3/2}. \tag{13}$$

In this relation, the approximative resonance condition

$$B_o \text{ [kG]} = 0.357\,\gamma f[\text{GHz}] \tag{14}$$

has been used. The magnetic compression g_c is defined as the ratio of the magnetic field at the interaction region to the magnetic field at the cathode, $g_c = B_o/B_k$. The relation (13) shows that the magnetic compression g_c should increase with increasing operating frequency in order to maintain an electric field E_k low compared to the breakdown value (≥ 80 kV/cm). Within this limit, the perpendicular velocity of the electrons could be increased by increasing the magnetic compression or the electric field at the cathode.

Another useful relation between the current density at the cathode j_k and the current density within the interaction region j can be found by using the Busch theorem together with the conservation of the electron current:

$$j = j_k g_c/\sin\phi_k, \tag{15}$$

where ϕ_k is the half-angle of the cathode. Assuming a cathode half-angle of 30°, a cathode current density $j_k = 6\,\text{A/cm}^2$ and a magnetic compression $g_c = 30$, Eq.(15)

yields at the interaction region a current density $j = 360$ A/cm^2 which is still far below the current density above which AC space charge effects become important [10]. Note that from Eq.(13), the electric field at the cathode is still modest (59 kV/cm) for $g_c = 30$, $\alpha = 1.5$, $V_c = 90$ kV and $f = 150$ GHz. Operating at higher frequencies requires higher voltage and/or larger magnetic compression in order to maintain a low electric field at the cathode.

The final consideration in this analysis is associated with the size of the electron beam. Because the current density j is rather limited by the previous considerations (magnetic compression, AC space charge effects), the cross-section of the beam has to be increased to obtain high current beam required by high power gyrotrons. To achieve this, one could increase the diameter of the annular beam or its thickness. Numerical calculations indicate however, that the perpendicular efficiency is more affected by a *large diameter thin* beam than a *small thick* one, because of the finite spot size of the radiation beam within the quasi-optical resonator.

To summarize, Table 2 shows the estimates of the gun parameters for a 150 GHz, 1 MW gyrotron. These values will serve as a guideline for a more accurate gun design based on trajectory simulations that will be presented in the next section.

2. Numerical simulations

A major task in this design phase is to select the shape of the electrodes in the gun emitter region. This can be done by using the *electrode synthesis* described in refs.[14, 15] and the cathode parameters listed in Table 2. An advantage of this method is that the electron beam produced from the synthesized gun is automatically laminar.

The next step is to trace numerically the electron trajectories from the emitter to the interaction region, using the EGUN code [16]. In these calculations, the external static magnetic field required to adiabatically compress the beam, was computed by a magnetic field code which solves the Biot-Savart equations. Further shaping of the synthesized electrodes were made to optimize the beam quality within the interaction region. In addition, the optimized position of the gun emitter with respect to the magnetic coils was searched. The final beam parameters (averaged value of α and velocity spreads at the interaction region) are plotted versus the control electrode voltage V_e in Fig.(6). These curves were obtained with a beam current $I = 50$ A and a cathode voltage $V_c = 90$ kV. At $V_e = 40$ kV, they show that an averaged α of 1.5 can be achieved with spreads in $\beta_\perp$ and $\beta_\parallel$ equal to 3.9% and 9.2% respectively. Higher values of α were also obtained with increasing V_e, without any observed mirror effects. At $V_e = 40$ kV, the maximum electric field at the gun emitter is 65 kV/cm, which is only 10% higher than the value predicted by the adiabatic theory, while the voltage depression $\Delta V/V$ is 4.2%, in good agreement with the value listed in the first column of Table 1.

In summary, we have demonstrated by numerical simulations, the feasibility of a MIG with performance parameters required by a 150 GHz, 1 MW quasi-optical gyrotron. Since the gun parameters for $f = 280$ GHz (or even higher) at the same power level are not much different from those required by $f = 150$ GHz, the same conclusion still applies. On the other hand, a more extensive study has to be done for guns which can be utilized in quasi-optical gyrotrons operating in the multi-megawatt power level, because of the higher values for both beam current and voltage.

V. Magnets

The superconducting magnets for high frequency quasi-optical gyrotron are of higher complexity than the one used by conventional gyrotrons. Their design must accomodate for a cross bore where the electromagnetic radiation can propagate without being influenced by the metallic boundary conditions. The free diameter of the cross bore must be at least four times the radiation beam waist everywhere in the resonator. The most frequent design [17–18] uses split coils with a free cross bore satisfying the above criterion. Whereas a Helmholtz pair would yield the most homogeneous axial field profile along the interaction region, the corresponding current density in the coils and the field at the inner coil surface may be too high to be compatible with the specifications of the existing superconductors.

We have conducted a design study of a magnet system [19] analogous to the one in Ref.[18], at a field compatible with the operation at 150 GHz. With the selected parameters ($\mu = 17$, $F = 0.12$, $\eta_{\perp} = 0.7$), the normalized detuning Δ is 0.5, and the corresponding magnetic field is 6.0 T in the interaction region. The cross bore diameter is fixed to 8 cm. The study pointed out that special care has to be provided in the cooling of the inner layers of the coils where the magnetic field could be as high as 8.6 T and where a bath cooling of the conductor is generally impossible. With this in consideration, such a coil system is technically feasible with the NbTi technology.

Scaling the design to the 280 GHz range requires the use of A-15 conductors since the field on the conductor exceeds the critical field of NbTi. Such a coil system would necessitate some technological development but it is considered within the present state of the art in the field [20]

VI. Conclusion

In this paper, a parametric analysis has been conducted to investigate the power capabilities of high frequency quasi-optical gyrotrons. The model employed is based on the single mode interaction between the electron beam and the TEM_{00} Gaussian radiation field within the resonator. Constraints on the beam and the resonator, such as the ohmic losses on the mirrors and the DC space charge effects within the beam are taken into account as required by long-pulse or cw operations. From the analysis, it was shown that output powers in excess of 1 MW are possible at 150 GHz and 280 GHz, with an energy extraction efficiency of about 20%. This relatively modest efficiency is due primarily to the annular shape of the electron beam. It could be somewhat improved by using a "pencil" or "sheet" beam. However, uncertainties of producing such beams having large currents still remain. In addition, a two-steps design study of a Magnetron Injection Gun for a 150 GHz, 1 MW quasi-optical gyrotron has been carried out, based on adiabatic theory and numerical simulations. It shows that the performances of the compressed electron beam are still good although the quasi-optical gyrotron requires a relatively thick beam.

References

[1] K. Felch, R. Bier, L. J. Crag, H. Huey, L. Yves, H. Jory, N. Lopez, S. Spang, *Int. J. Electron.*, **61**, 701(1986).

[2] K. E. Kreischer, R. J. Temkin, *Phys. Rev. Lett.*, **59**, 547(1987).

[3] P. Sprangle, J. L. Vomvoridis, W. M. Manheimer, *Phys. Rev. A,* **23**, 3121(1981).

[4] V. A. Flyagin, A. L. Goldenberg, N. S. Nusinovich, *in Infrared and Millimeter Waves, K. J. Button, editor,* **11**, 179(1984).

[5] B. G. Danly, R. J. Temkin, *Phys. Fluids,* **29**, 561(1986).

[6] T. M. Tran, B. G. Danly, K. E. Kreischer, J. B. Schutkeker, R. J. Temkin, *Phys. Fluids,* **29**, 1274(1986).

[7] A. Bondeson, W. M. Manheimer, E. Ott, *in Infrared and Millimeter Waves, K. J. Button, editor,* **9**, 309(1983).

[8] A. G. Luchinin, G. S. Nusinovich, *Int. J. Electron.,* **57**, 827(1984).

[9] A. K. Ganguly, K. R. Chu, *Int. J. Infr. and Mm. Waves,* **5**, 103(1984).

[10] K. E. Kreischer, B. G. Danly, J. B. Schutkeker, R. J. Temkin, *IEEE Trans. Plasma Sci.,* **13**, 364(1985).

[11] A. Perrenoud, T. M. Tran, M. Q. Tran, C. Rieder, M. Schleipen, A. Bondeson, *Int. J. of Electron.*, **57**, 985(1984).

[12] M. Q. Tran, A. Bondeson, A. Perrenoud, S. Alberti, B. Isaak, P. Muggli, *Int. J. of Electron.,* **61**, 1041(1986).

[13] A. L. Goldenberg, M. I. Petelin, *Radiophys. Quant. Electron.,* **15**, 106(1976).

[14] V. N. Manuilov, Sh. H. Tsimring, *Radiophys. Quant. Electron.,* **23**, 111(1978).

[15] A. W. Fliflet, A. J. Dudas, M. E. Read, J. M. Baird, *Int. J. of Electron.,* **53**, 743(1982).

[16] W. B. Herrmannsfeldt, SLAC-Report 226, (1979).

[17] M. Q. Tran and the Lausanne Quasi-Optical Gyrotron Development Group, *Proc. 5th Int. Workshop on ECE and ECH, San Diego*, 294(1986).

[18] M. E. Read, M.Q. Tran, J. Mc. Adoo, M. Barsanti, *to be published in Int. J. Electronics,* **64**, (1988).

[19] A. Perrenoud, M. Q. Tran, P. Muggli, Lausanne CRPP Internal Report Int. 126/86 (unpublished).

[20] G. Vecsey, K. Kwasnitza, Paul Scherrer Institute, Villigen (Switzerland), Private communication.

	$f = 150$ GHz $P = 1$ MW	$f = 280$ GHz $P = 1$ MW	$f = 150$ GHz $P = 5$ MW
V_c (kV)	90.2	81.0	123
I (A)	49.0	54.1	181
$\beta_\perp$	0.441	0.423	0.505
$\beta_\parallel$	0.271	0.253	0.250
I_{MAX} (A)	142	123	214
$\Delta V/V$ (%)	4.3	5.6	12.6
η	0.24	0.23	0.22
$g = 1 - d/R$	−0.64	−0.90	−0.85
d/λ	190	399	155
T (%)	8.5	10.7	29.4

Table 1. Design parameters for quasi-optical gyrotrons with $F = 0.12$, $\mu = 17$, $\eta_\perp = 0.35$, $\rho_{\mathrm{ohm}} = 1.5\ \mathrm{kW/cm^2}$, $\sigma = 3.6 \times 10^7\ \Omega^{-1}\mathrm{m}^{-1}$ and $R_e/R_w = 0.7$.

Interaction region	
$\beta_\perp$	0.441
$\beta_\parallel$	0.271
Magnetic field (T)	6.26
Cathode voltage (kV)	90
Current (A)	50
Current density $(A/cm)^2)$	360
Averaged beam radius (cm)	0.235
Beam Thickness (cm)	0.094
Cathode region	
Magnetic field (T)	0.21
Electric field (kV/cm)	59
Current density (A/cm^2)	6
Maximum emitter radius (cm)	1.55
Emitter length (cm)	1.03
Emitter half-angle	30

Table 2. Design beam parameters for a 1 MW, 150 GHz quasi-optical gyrotron.

Figure Captions

Fig. 1 Perpendicular efficiency for a *pencil* beam, versus the normalized interaction length μ and the normalized field amplitude F.

Fig. 2 The ohmic constraints on the normalized field amplitude F and the maximum cathode voltage for $\rho_{\mathrm{ohm}} = 1.5\ \mathrm{kW/cm^2}$, at 150 GHz.

Fig. 3 The limiting electron beam power versus the beam voltage, assuming $R_e/R_w = 0,7$, for several values of α.

Fig. 4 The permissible beam and resonator paramaters for a 150 GHz quasi-optical gyrotron, versus the output power, assuming $F = 0.12$, $\mu = 17$, $\eta_\perp = 0.35$, $\rho_{\mathrm{ohm}} = 1.5\ \mathrm{kW/cm^2}$ and $R_e/R_w = 0.7$:

(a) The cathode voltage.

(b) The electron beam current.

(c) The mirror curvature parameter $1 - g$.

(d) The mirror spacing normalized to the wavelength.

(e) The resonator two-way transmission losses.

Fig. 5 The permissible beam and resonator paramaters for a 280 GHz quasi-optical gyrotron, versus the output power, assuming $F = 0.12$, $\mu = 17$, $\eta_\perp = 0.35$, $\rho_{\mathrm{ohm}} = 1.5\ \mathrm{kW/cm^2}$ and $R_e/R_w = 0.7$:

(a) The cathode voltage.

(b) The electron beam current.

(c) The mirror curvature parameter $1 - g$.

(d) The mirror spacing normalized to the wavelength.

(e) The resonator two-way transmission losses.

Fig. 6 The beam characteristics at the interaction region, obtained from trajectory numerical simulations, for a 90 kV, 50 A electron beam.

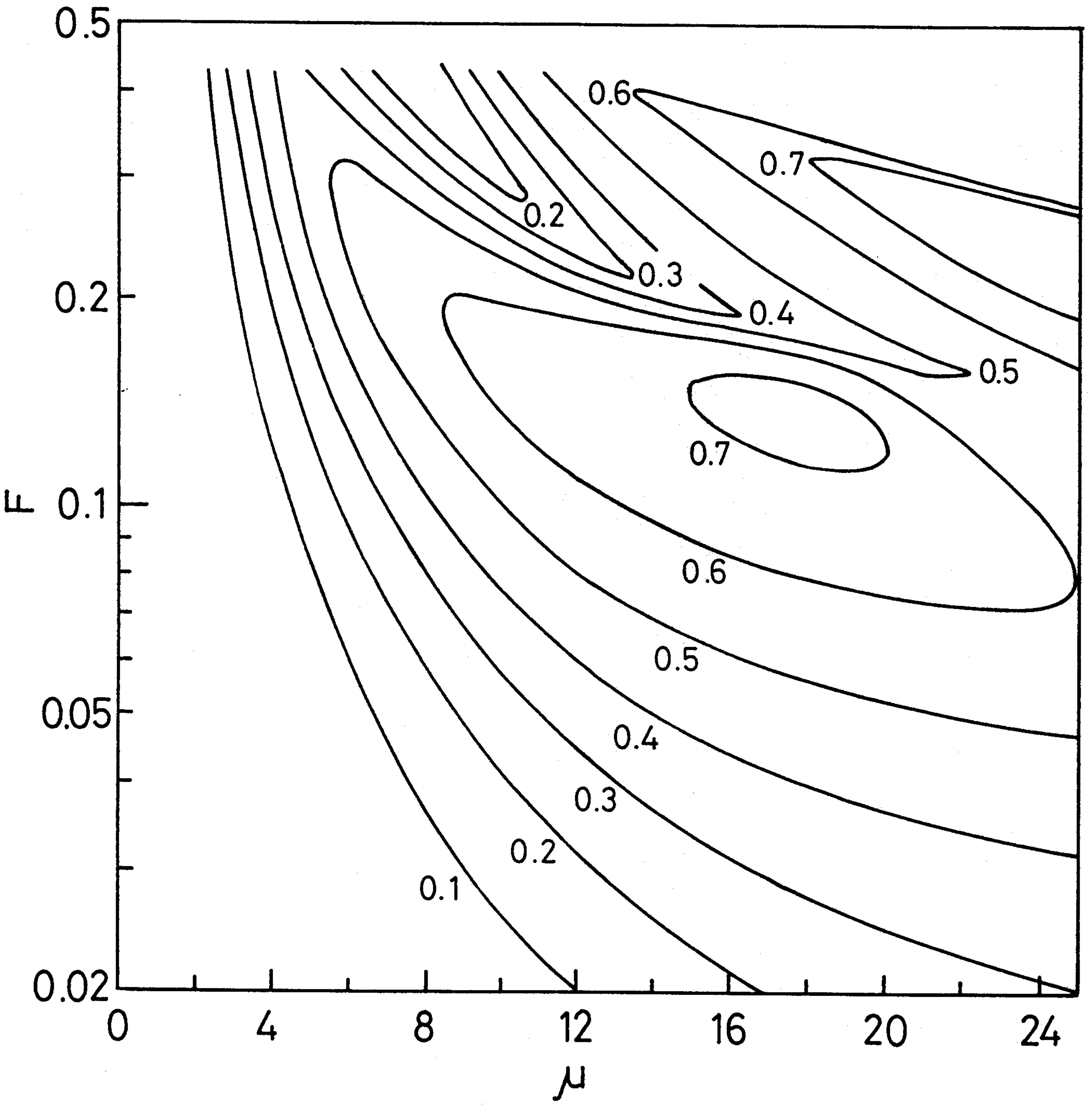
0.5
0.2
0.1
0.05
0.02
F
0
4
8
12
16
20
24
μ
0.6
0.7
0.2
0.3
0.4
0.5
0.7
0.6
0.5
0.4
0.3
0.2
0.1

Figure 1

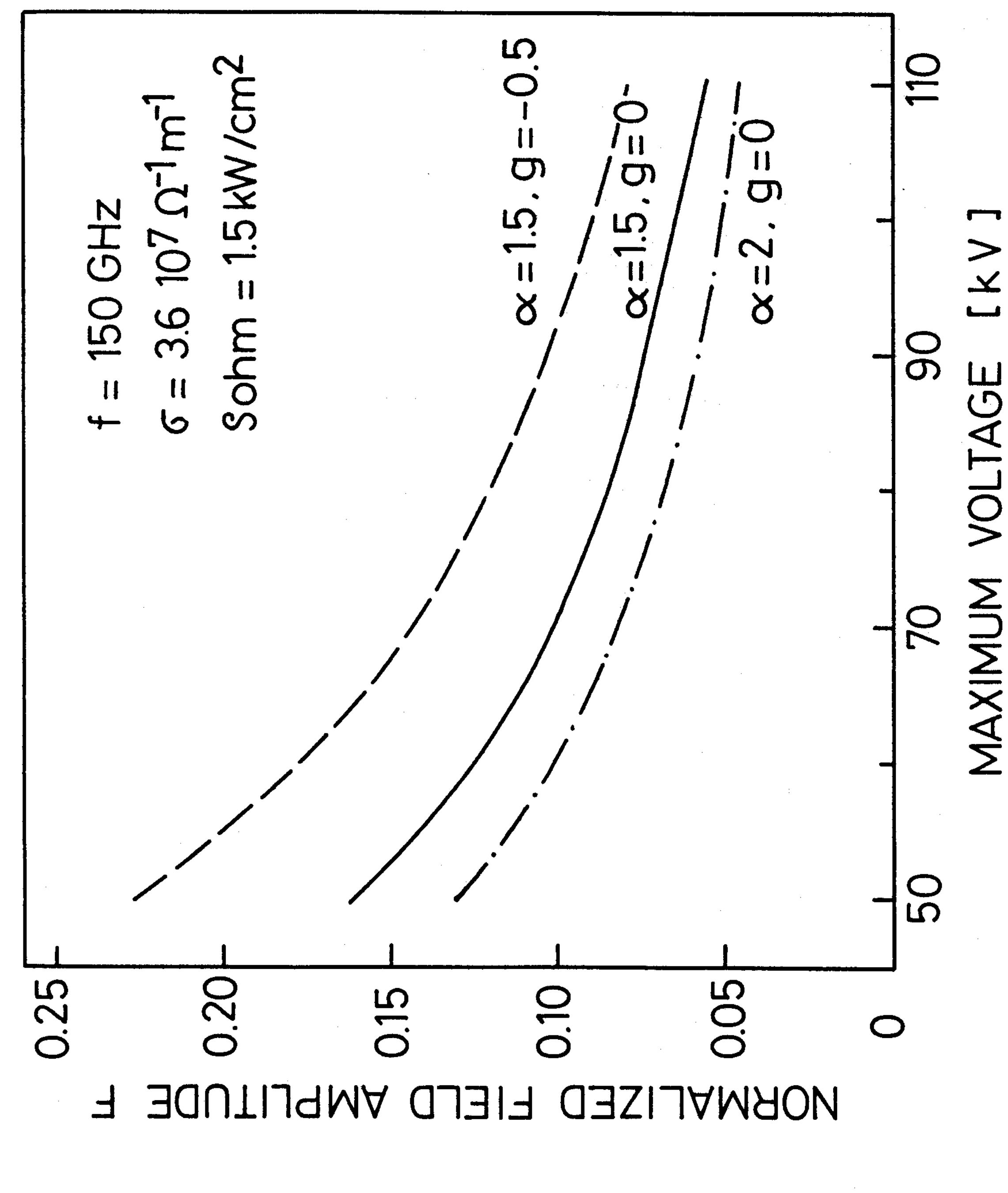

f = 150 GHz
σ = 3.6 10^7 Ω^-1 m^-1
Sohm = 1.5 kW/cm^2
α=1.5, g=-0.5
α=1.5, g=0
α=2, g=0
50
70
90
110
MAXIMUM VOLTAGE [kV]
0
0.05
0.10
0.15
0.20
0.25
NORMALIZED FIELD AMPLITUDE F

Figure 2

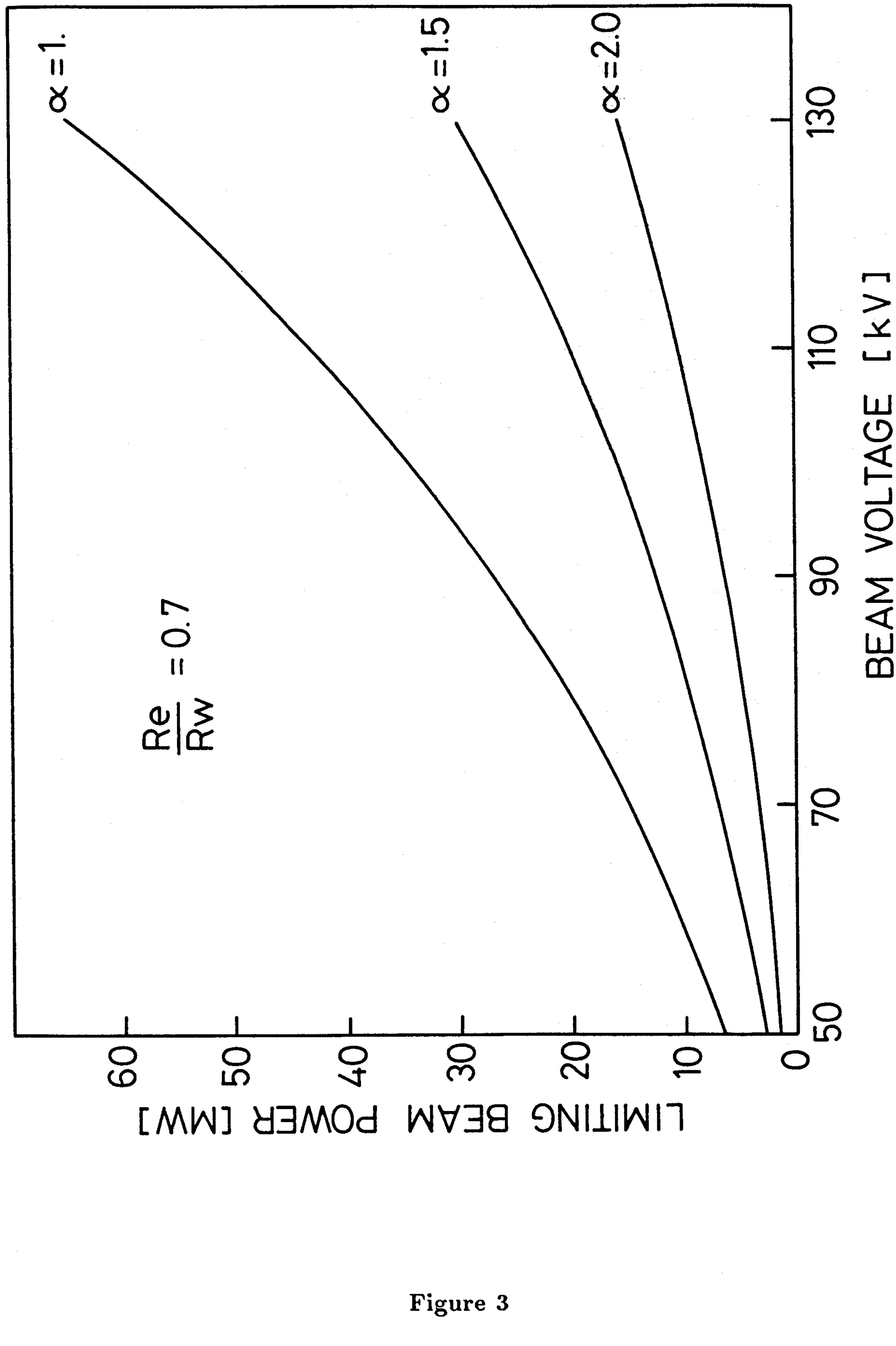

LIMITING BEAM POWER [MW]
0
10
20
30
40
50
60
BEAM VOLTAGE [kV]
50
70
90
110
130
$\frac{Re}{Rw} = 0.7$
α = 1.
α = 1.5
α = 2.0

Figure 3

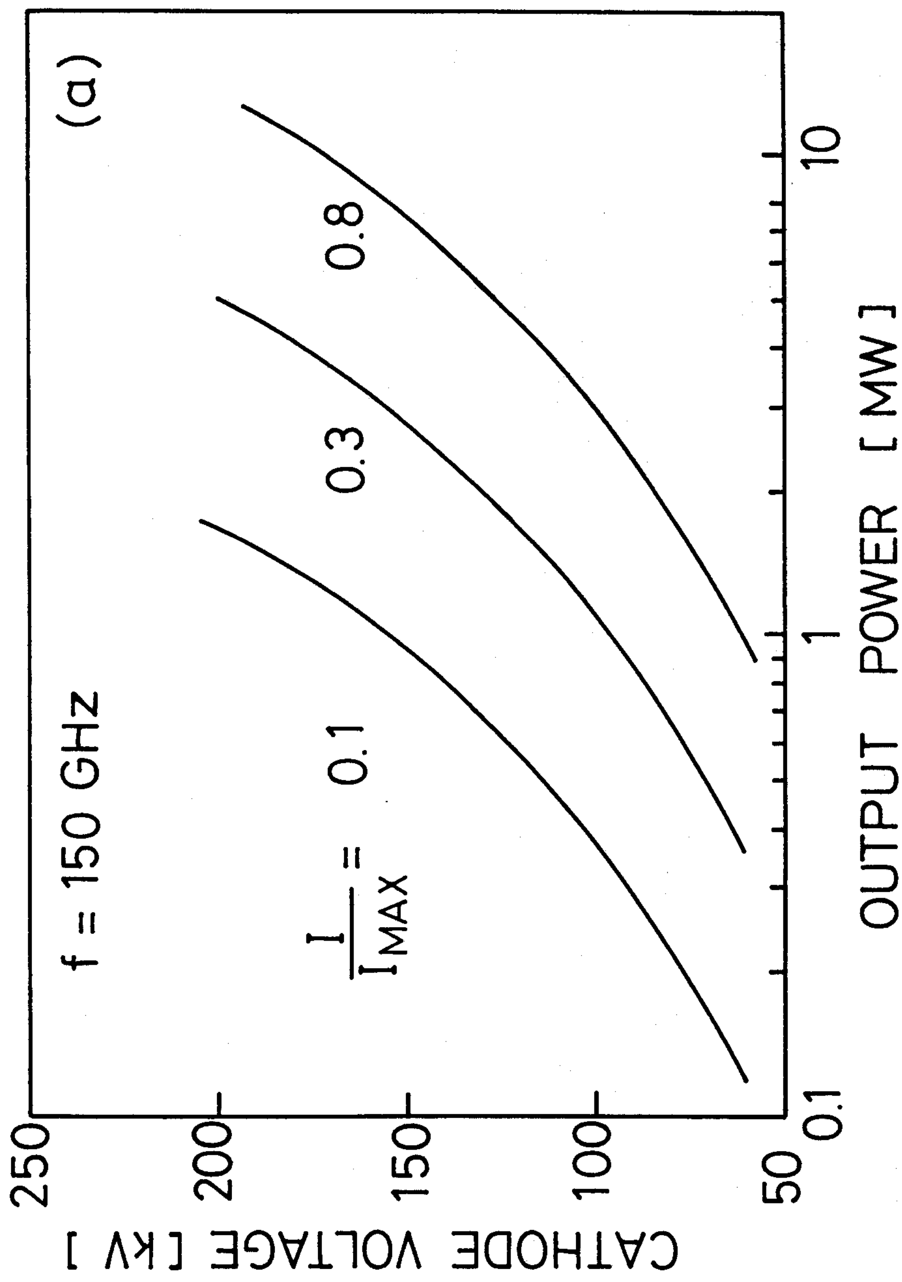
f = 150 GHz
(a)
I/I_MAX =
0.1
0.3
0.8
OUTPUT POWER [MW]
CATHODE VOLTAGE [kV]
250
200
150
100
50
0.1
1
10

Figure 4.a

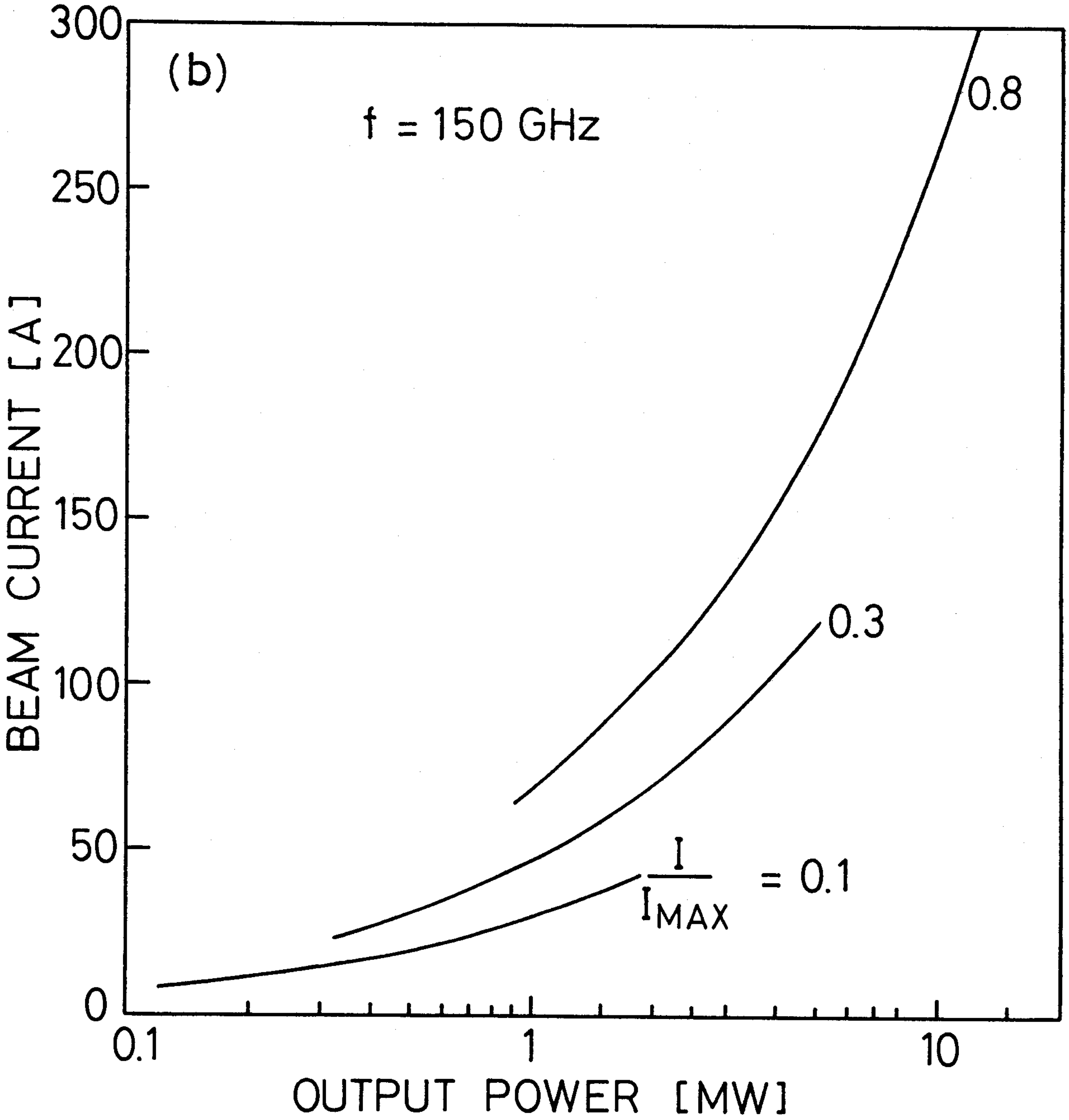

(b)
f = 150 GHz
0.8
0.3
$\frac{I}{I_{MAX}}$ = 0.1
BEAM CURRENT [A]
OUTPUT POWER [MW]
300
250
200
150
100
50
0
0.1
1
10

Figure 4.b

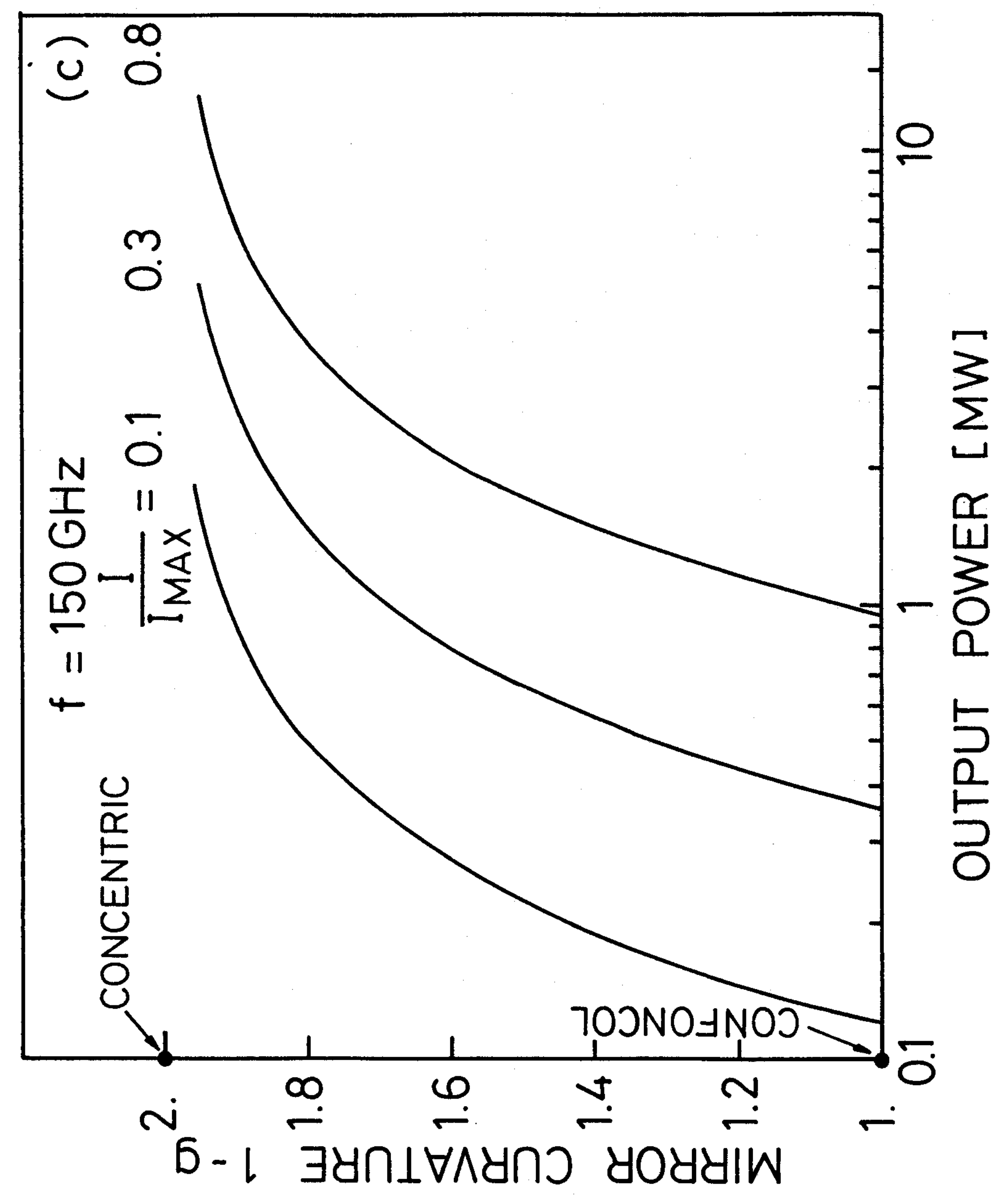

(c)
f = 150 GHz
I / I_MAX = 0.1
0.3
0.8
CONCENTRIC
CONFONCOL
MIRROR CURVATURE 1 - g
2.
1.8
1.6
1.4
1.2
1.
0.1
1
10
OUTPUT POWER [MW]

Figure 4.c

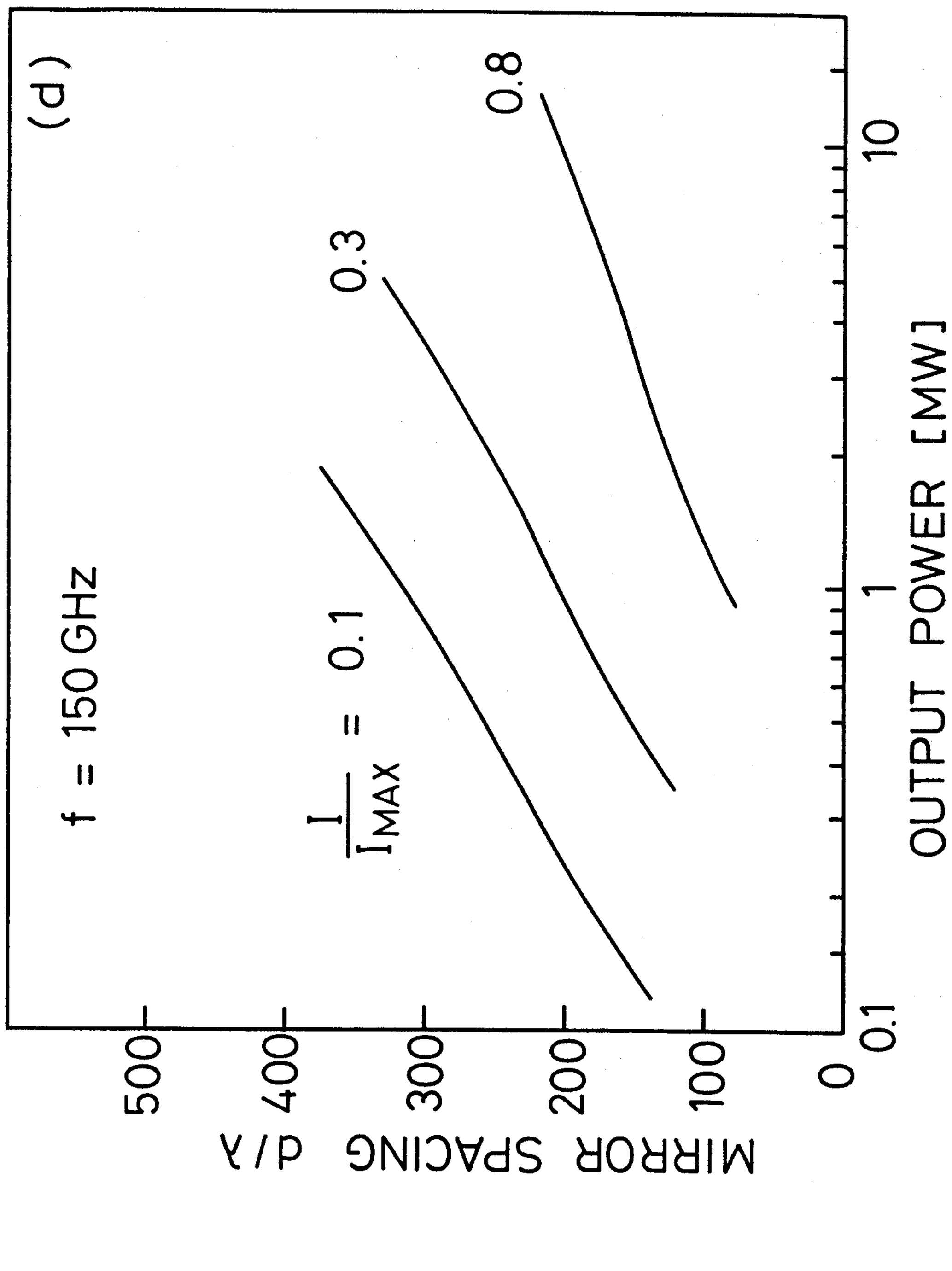

(d)
f = 150 GHz
$\frac{I}{I_{MAX}}$ = 0.1
0.3
0.8
MIRROR SPACING d/λ
OUTPUT POWER [MW]
0
100
200
300
400
500
0.1
1
10

Figure 4.d

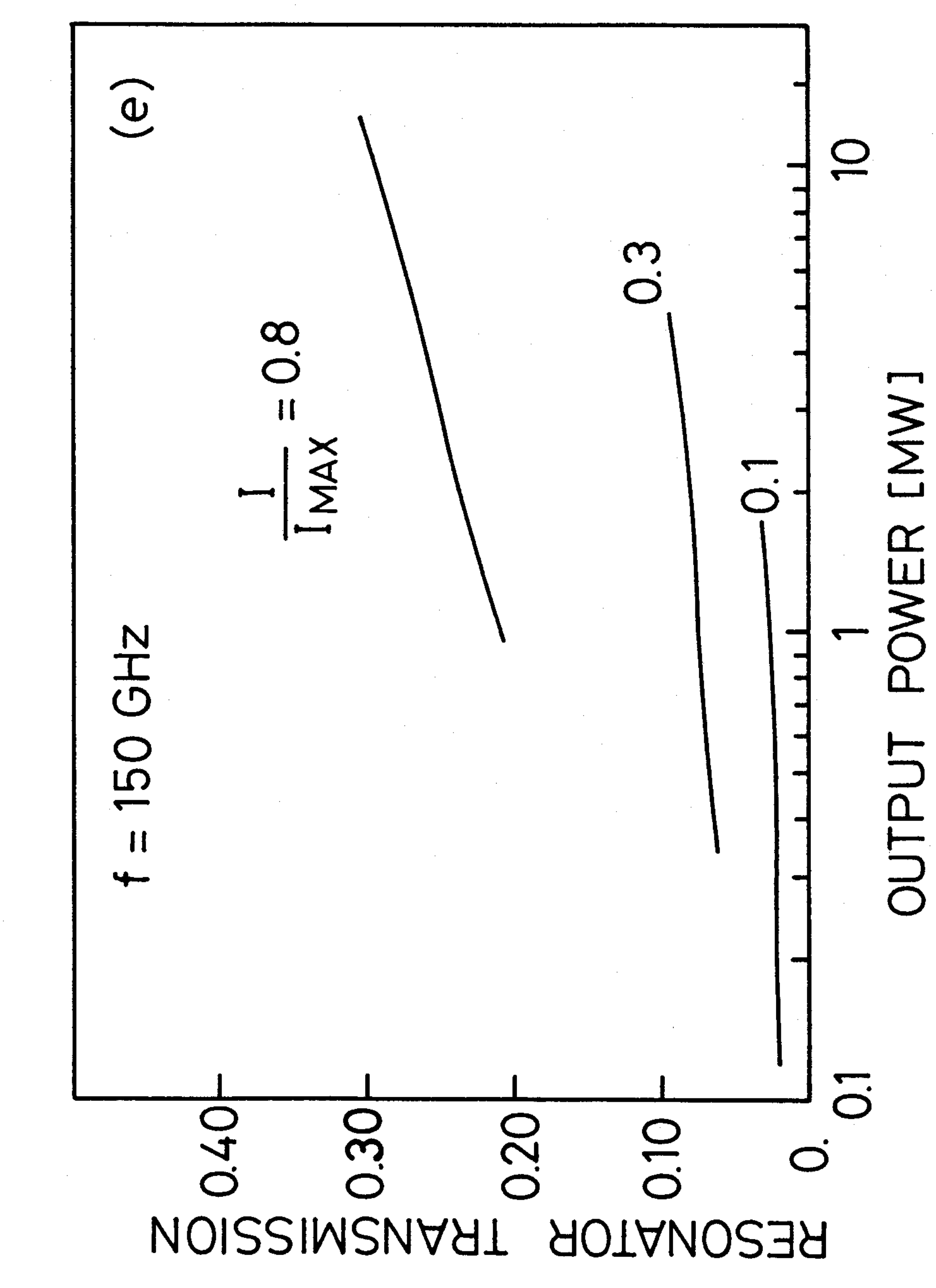

RESONATOR TRANSMISSION
0. 0.10 0.20 0.30 0.40
OUTPUT POWER [MW]
0.1 1 10
f = 150 GHz
(e)
$\frac{I}{I_{MAX}} = 0.8$
0.3
0.1

Figure 4.e

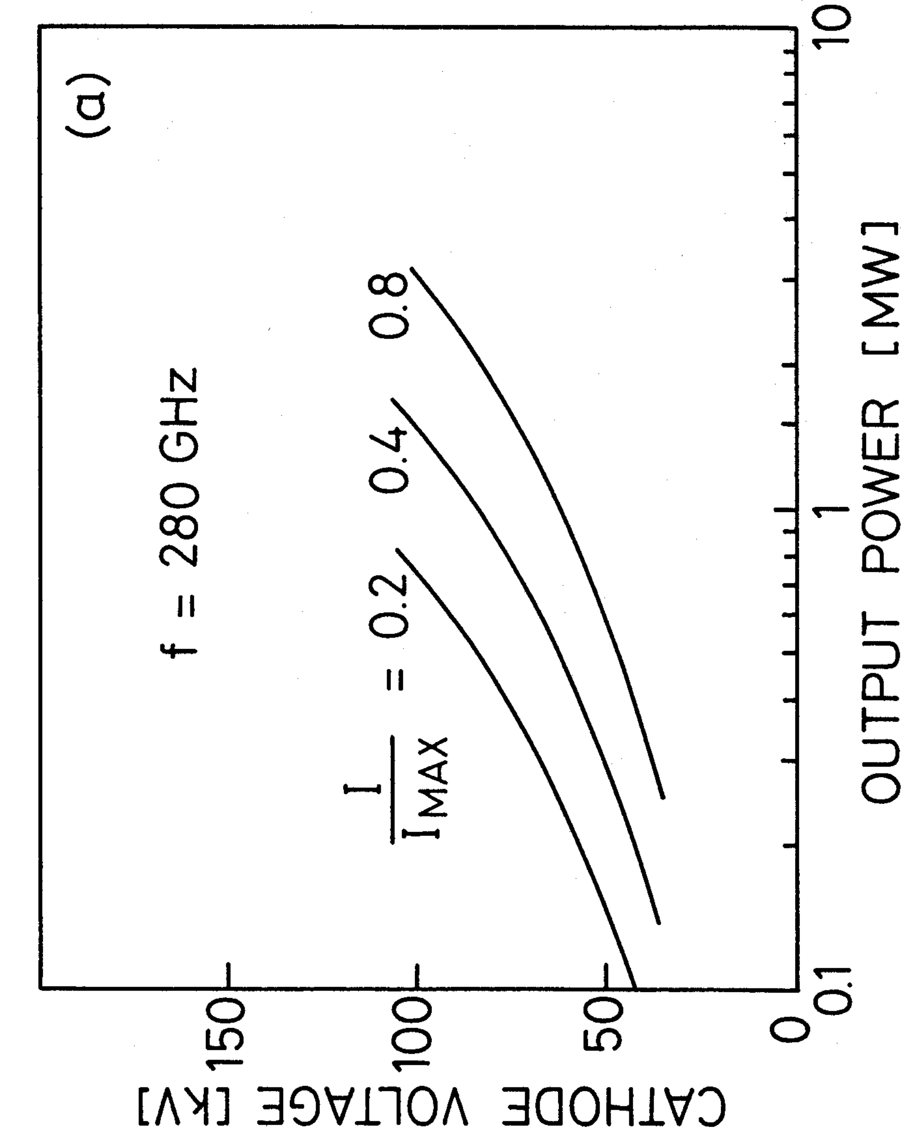

(a)
f = 280 GHz
I / I_MAX = 0.2 0.4 0.8
CATHODE VOLTAGE [KV]
0
50
100
150
OUTPUT POWER [MW]
0.1
1
10

Figure 5.a

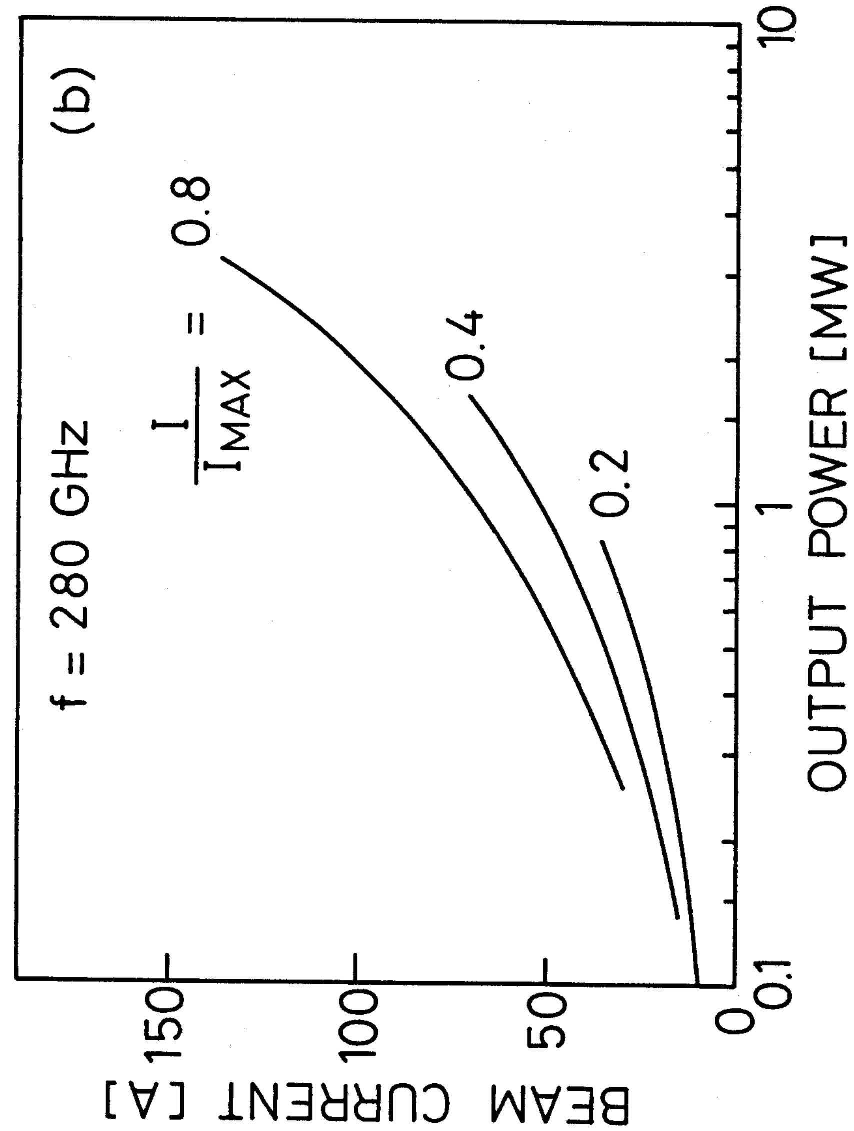

f = 280 GHz
(b)
I/IMAX = 0.8
0.4
0.2
OUTPUT POWER [MW]
BEAM CURRENT [A]
0
50
100
150
0.1
1
10

Figure 5.b

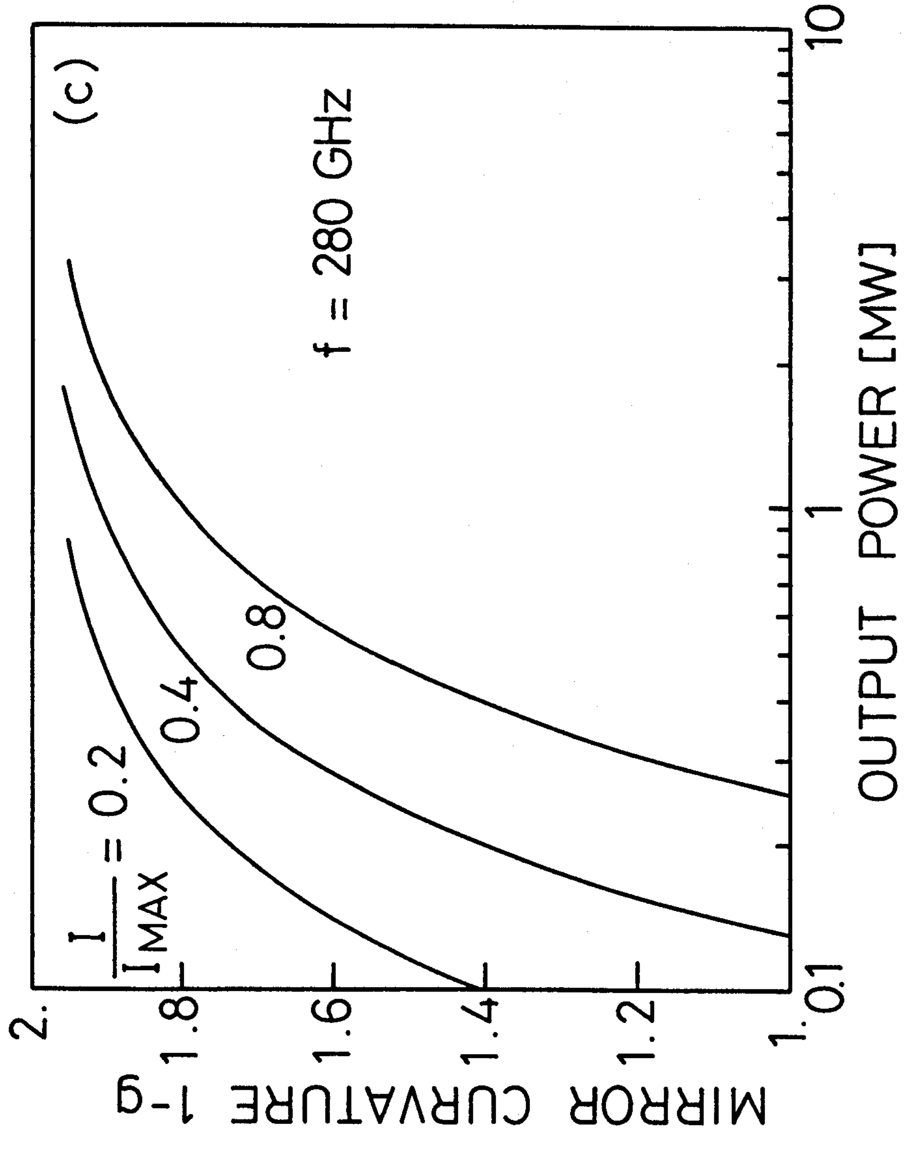

(c)
f = 280 GHz
I/I_MAX = 0.2
0.4
0.8
2.
1.8
1.6
1.4
1.2
1.
0.1
1
10
MIRROR CURVATURE 1-g
OUTPUT POWER [MW]

Figure 5.c

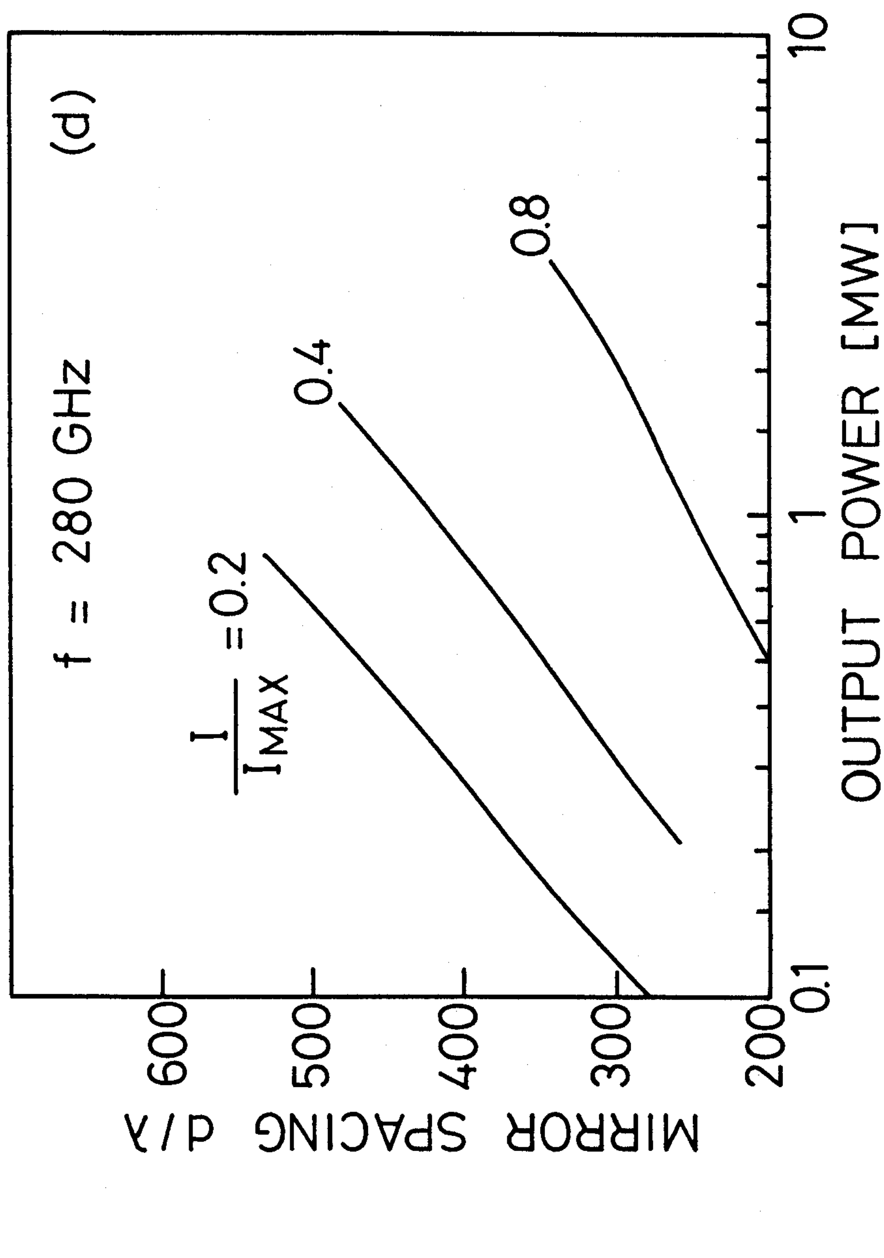

f = 280 GHz
(d)
I / I_MAX = 0.2
0.4
0.8
MIRROR SPACING d/λ
200
300
400
500
600
0.1
1
10
OUTPUT POWER [MW]

Figure 5.d

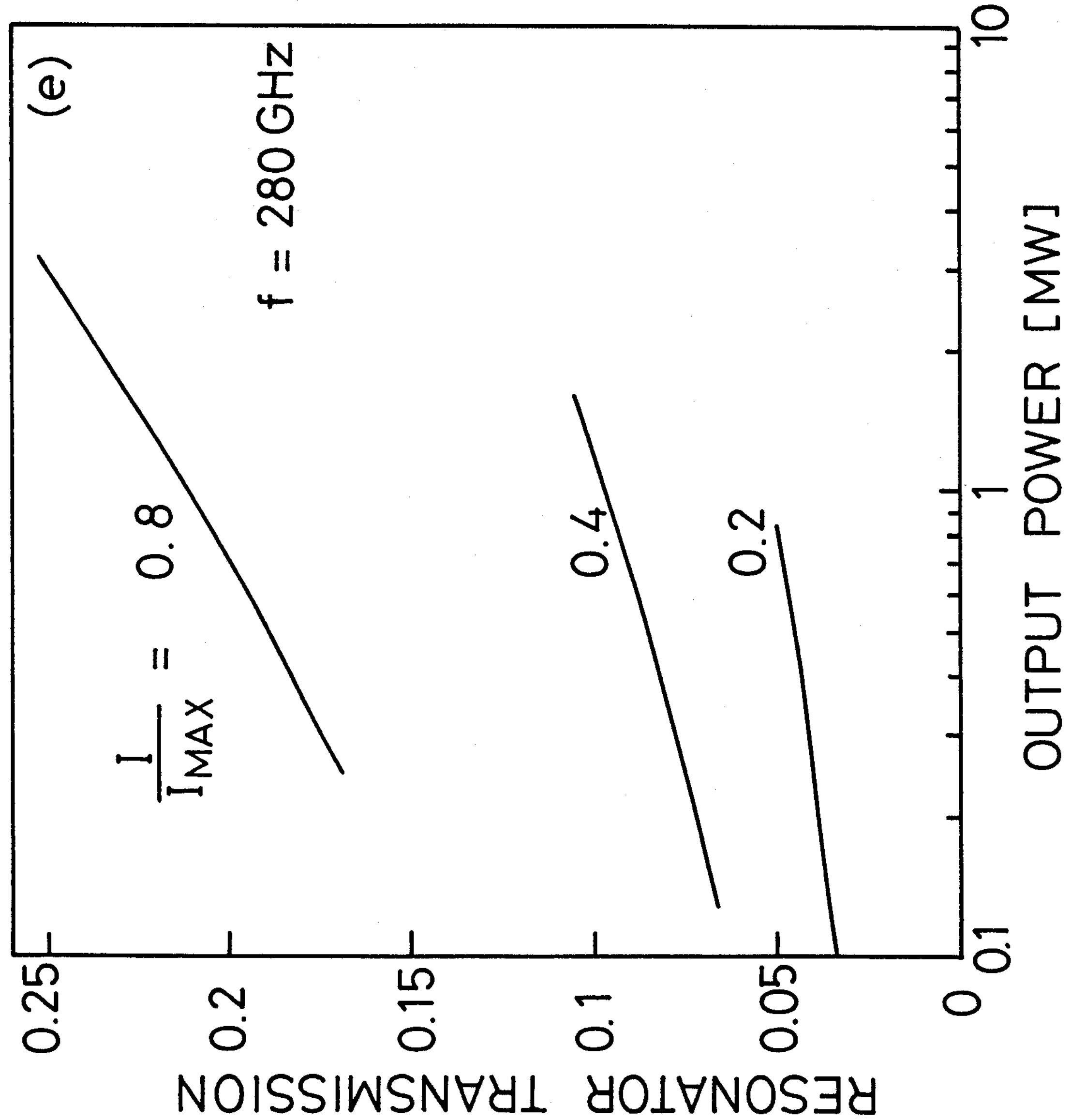

(e)
f = 280 GHz
I/I_MAX = 0.8
0.4
0.2
0.25
0.2
0.15
0.1
0.05
0
0.1
1
10
RESONATOR TRANSMISSION
OUTPUT POWER [MW]

Figure 5.e

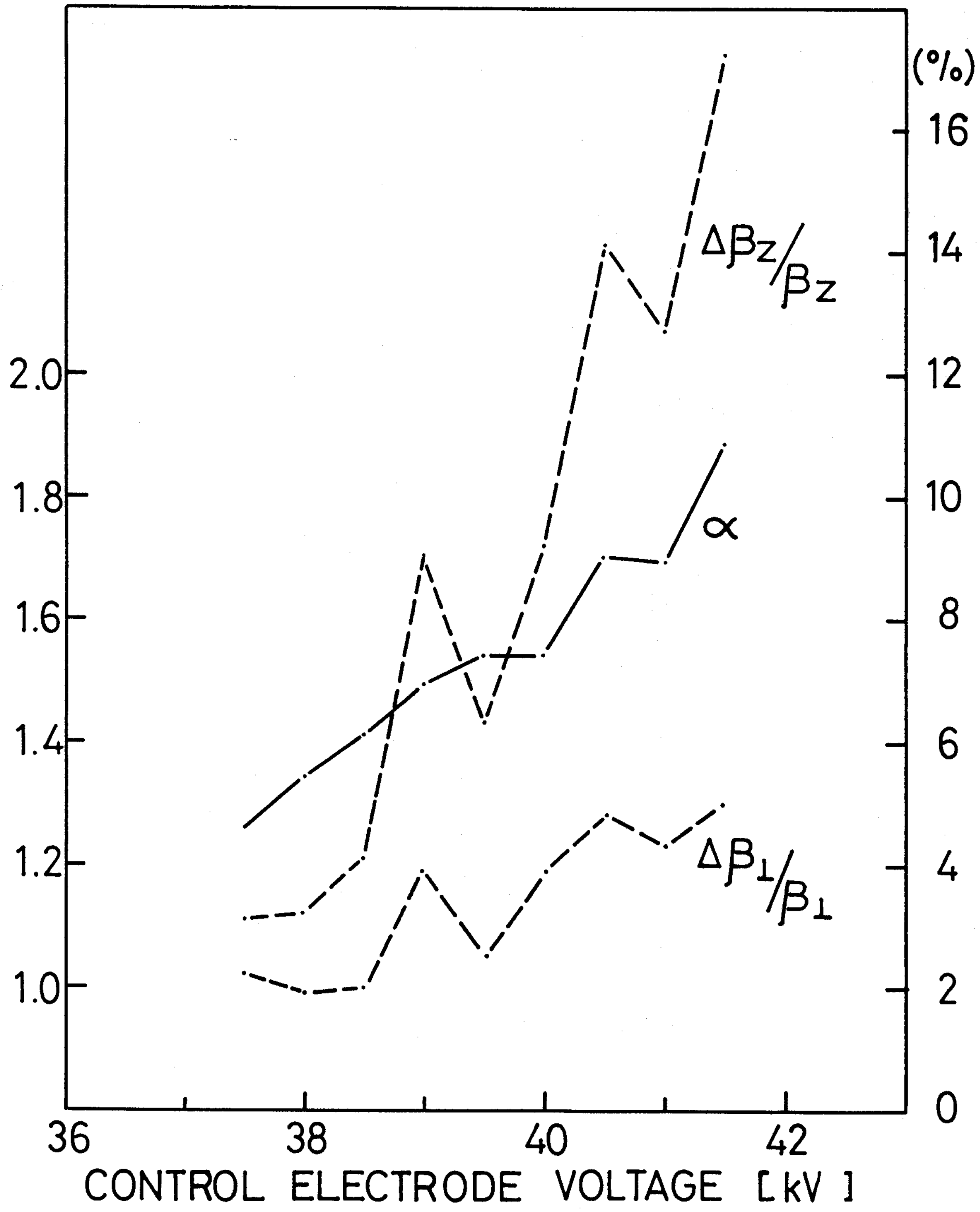
(%)
16
14
12
10
8
6
4
2
0
2.0
1.8
1.6
1.4
1.2
1.0
$\Delta\beta_z/\beta_z$
α
$\Delta\beta_\perp/\beta_\perp$
36
38
40
42
CONTROL ELECTRODE VOLTAGE [kV]

Figure 6